Asymmetric line broadening in intracavity loss modulated quantum well distributed feedback lasers

J. O'Gorman, A. F. J. Levi, T. Tanbun-Ek, and R. A. Logan
AT&T Bell Laboratories, Murray Hill, New Jersey 07974

(Received 2 August 1990; accepted for publication 14 November 1990)

We report for the first time high-speed (Gbit s^{-1}), single mode, digital (on-off) modulation of intracavity loss modulated 1.55 μm InGaAs/InP multiple quantum well distributed feedback lasers. The lasing spectrum, observed to be asymmetrically broadened under high-speed modulation, is shown to result from large carrier density variations which accompany this switching scheme. We also show, for the first time, digitally current-modulated lasers have broader linewidths than devices which use intracavity loss modulation.

Recently we have considered lasers with intracavity loss modulators for digital optoelectronic signal processing. Voltage-controlled Q switching[1] and digital logic operation[2] at high bit rates have been demonstrated. This study illustrated the importance of digital (on-off) Fabry–Perot devices for short haul (<1 km) applications. For longer distance communications (for example, local area networks) the effect of fiber dispersion dictates that optical sources of greater spectral purity such as distributed feedback (DFB) lasers be used. It is well known that dynamic spectral broadening (or chirp) is an important factor affecting performance, especially in digital (on-off) modulation schemes.[3] In this letter we report on the spectral behavior of DFB lasers with an intracavity loss modulator under high-speed (Gbit s^{-1}) digital (on-off) data transmission. These devices emit at a wavelength of 1.55 μm, lasing in a single longitudinal mode which is asymmetrically broadened at high modulation rates. We show this broadening is due to large carrier density variations which accompany the switching process.[4] We calculate the time-averaged power spectrum of the laser and obtain good agreement with experiment. These results are also compared with those obtained using conventional current modulation.

The laser structures used were InGaAs/InP buried-heterostructure multiple quantum well graded index separate confinement heterostructure distributed feedback (BH-MQW-GRINSCH-DFB) lasers grown by atmospheric pressure metalorganic vapor phase epitaxy (MOVPE) on a first-order grating prepared on a ⟨100⟩ oriented n-type InP substrate.[5] After introduction of the wafer into the growth chamber the substrate temperature was increased to 625 °C in an AsH_3/PH_3 gas flow to protect the gratings from erosion. Undoped step graded index layers of band gap 1.08 (100 nm thick), 1.16, and 1.25 μm (each of thickness 25 nm) were first deposited followed by four 5-nm-thick $In_{0.53}Ga_{0.47}As$ quantum wells separated by 22.5-nm-thick barrier layers of band gap 1.25 μm. The upper part of the graded index, similar to the lower one but with an increasing band gap, was then grown. Finally a 2-μm-thick p-type InP cladding layer and a 120-nm-thick p^+-InGaAsP contact layer were deposited. After crystal growth, BH lasers were formed by mesa stripe etching, the width of the active region was then reduced using a selective etch, and finally semi-insulating Fe-InP was regrown, using MOVPE. Using standard etching and metallization techniques, front-side electrical contact to the n^+ and p^+ layers is achieved resulting in the geometry shown in the inset of Fig. 1. The wafer is then cleaved yielding DFB lasers with a voltage-controlled saturable absorption section.

We have used these lasers as sources for medium-haul, high bit rate, digital signal transmission. The experimental arrangement is shown in Fig. 1. The laser is butt coupled to the cleaved end of an 8 km single-mode fiber and a 1 Gbit s^{-1} nonreturn to zero (NRZ) 2^{20}-1 pseudo random bit stream (PRBS) is applied to the absorber section. The optical signal is detected by a receiver with a 7 GHz bandwidth. In Fig. 2(a) we show the eye pattern obtained when the PRBS of Fig. 2(b) is applied to the absorber section. A well-defined eye is observed indicating little penalty due to laser chirp and fiber dispersion. The large eye opening is indicative of the high contrast ratio obtained by digital (on-off) intracavity absorption modulation. The received eye diagram shows asymmetric jitter in the rise (<200 ps) and fall (<100 ps) regimes. The larger jitter in the rise time is caused by variations in the turn-on delay since the laser is switched from below threshold. Subsequent NRZ bit error-rate measurements at 1 Gbit s^{-1} using 2^{20}-1 PRBS gave error rates of less than 10^{-12}.

We have also investigated the wavelength dependence of the optical output on bit rate. In Fig. 3 we show the development of the time-averaged laser spectrum with increasing modulation rate. A ...101010... bit stream applied to the absorber section produces the greatest spectral broadening. Smaller broadening is observed under PRBS modulation. As the bit rate is increased from static (dc) to 1 Gbit s^{-1} the full width half maximum (FWHM) spectral linewidth is observed to increase from 0.1 (instrument limited) to 0.13 nm. The FWHM of the laser line remains small even at these high modulation rates because of the intrinsically narrow line associated with QW-DFB structures.[6] However, a pronounced shoulder develops on the short-wavelength side of the main spectral peak with increasing bit rate. We demonstrate that this asymmetric broadening is due to the large carrier density variations

 0003-6951/91/070669-03$02.00

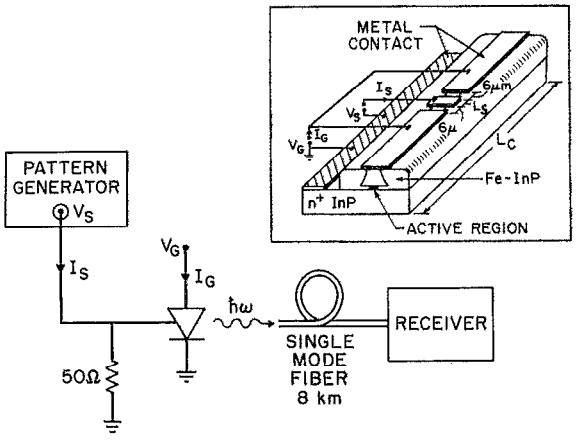

FIG. 1. Experimental arrangement. Inset shows schematic of a BH-MQW-GRINSCH-DFB laser diode with a cavity length L_c and an intracavity absorber of length L_s. The current into the long gain section is I_G, the absorber voltage and current are V_s and I_s, respectively.

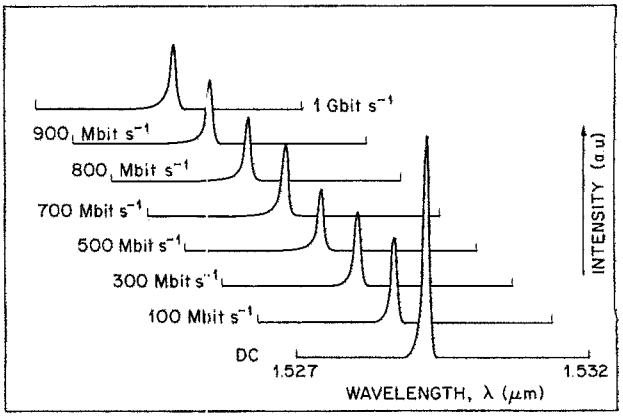

FIG. 3. Experimental time-averaged optical spectra recorded when a ...101010... data stream is applied to saturable absorber, S, at bit rates up to 1 Gbit s^{-1}. Gain current $I_G = 100$ mA.

which accompany the Q-switching process.[4]

The intracavity loss modulated laser is governed by a set of single-mode rate equations which may be written as[4]

$$\frac{dn}{dt}=\frac{I_G}{ev}-R, \tag{1}$$

$$\frac{dp}{dt}=\left(\Gamma G-\frac{1}{\tau_p'}\right)p+R_{\rm sp}, \tag{2}$$

where p is the photon density, n is the carrier density, R is the charge carrier recombination rate, G is the gain function, I_G is the gain current, $R_{\rm sp}$ is the spontaneous emission coupling into the lasing mode, v is the active region volume, Γ is the confinement factor, and $1/\tau_p'$ describes the total losses in the laser and may be written as

$$1/\tau_p'=(1/\tau_p)\left[1+r_1+r_2V_s+r_3/(1+I/I_s)\right], \tag{3}$$

where $1/\tau_p$ describes the familiar internal and mirror losses. V_s is the voltage applied to the absorbing segment, I_s is the absorption saturation intensity which increases with increasing reverse bias, and r_1, r_2, and r_3 are parameters describing the dependence of saturable and nonsaturable absorption on voltage for lasers of different geometries.

We have previously shown[4] that, when the absorption is switched by an applied voltage, the optical output of the multielectrode laser is accompanied by large and rapid variation in the carrier density. Consequently, large signal analysis is appropriate and requires numerical integration of Eqs. (1)–(3).

The spectrum was calculated by first integrating Eqs. (1)–(3) using standard parameter values.[4] Having obtained the carrier and photon densities, the variation in refractive index ($\Delta\mu$) is calculated assuming a linear dependence of carrier-induced refractive index change on carrier density ($\Delta\mu/\Delta n$). The effective change in refractive index also varies linearly with confinement factor (Γ) and so we use a reasonable value of -9×10^{-22} cm^3 for $\Gamma\Delta\mu/\Delta n$ (Ref. 7). In Fig. 4(a) we show the calculated spectrum of the laser when a 1 Gbit s^{-1}, ...101010... NRZ data stream is applied to saturable absorber S. Spectral broadening (FWHM = 0.01 nm) and in addition a broad shoulder situated on the short-wavelength side of the main mode is predicted in qualitative agreement with the experimental result of Fig. 3. This shoulder is seen to result from the large carrier density variation and optical overshoot that accompanies the switching process.

In Fig. 4 we also compare the spectral broadening which results from large signal modulation of conventional DFB lasers, using the same parameter values (with the exception of those describing the saturable and nonsaturable loss which are set to zero) as used in Fig. 4(a). To

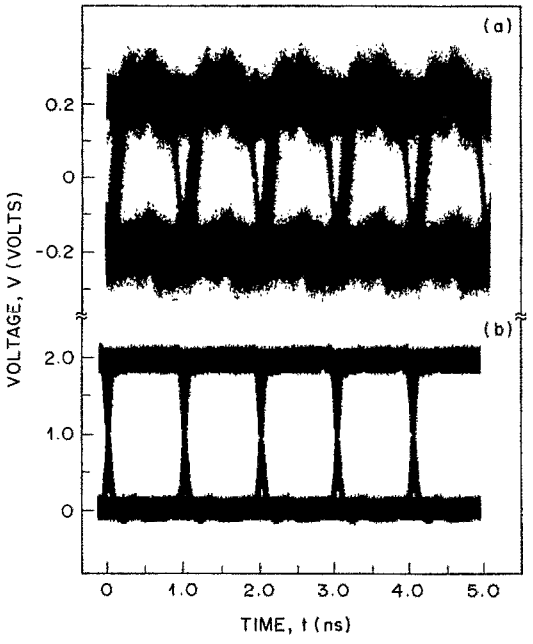

FIG. 2. (a) Received eye diagram for a 1 G bit s NRZ $2^{20}-1$ PRBS after transmission through 8 km of single-mode fiber, (b) eye diagram for voltage, V_s, applied to the absorber section.

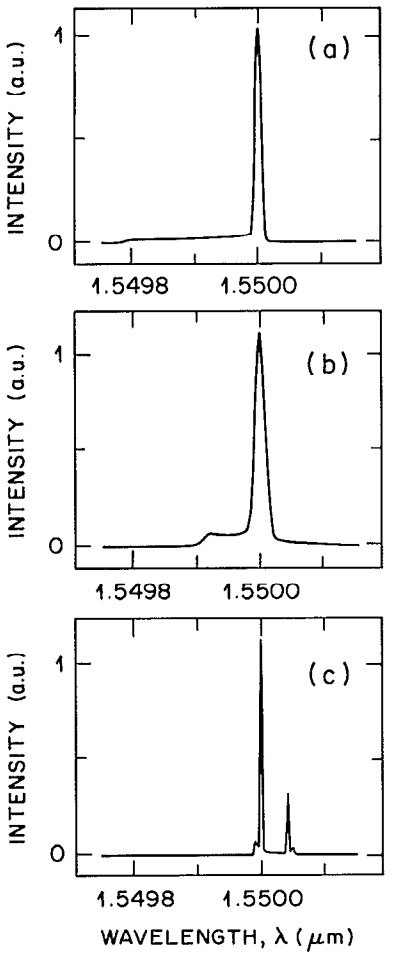

FIG. 4. Calculated time-averaged optical spectra when: (a) switching 2 mW of optical power per facet by application of a $0 < V_s < 1$ V ...101010... 1 Gbit s^{-1} data stream to an intracavity loss modulated DFB with $I_G = 45$ mA, (b) switching with the same bit pattern/rate as (a) 2 mW of optical power per facet from below threshold by application of 33 mA current pulses riding on a 20 mA dc bias current, (c) switching of 2 mW of optical power per facet by application of 19 mA current pulses with a laser dc bias current of 43 mA. In (b) and (c) the laser threshold was 35 mA.

achieve fair comparison between the two modulation schemes the switched optical powers are chosen to be equal. Figure 4(b) shows the calculated spectrum when the laser current is modulated from below threshold. Again a pronounced feature is evident on the short-wavelength side; however, the calculated spectral width is broader (FWHM $= 0.02$ nm) due to the relatively slow variation in the carrier density as the laser carrier density is increased above threshold. A common feature to both modulation schemes is that the laser is switched from the off to the on state leading to relaxation oscillations at the leading edge of the optical waveform. This leads to the broad feature on the short-wavelength side of the spectrum as during this portion of the optical waveform the carrier density decreases to the value at which it is pinned at laser threshold.

In Fig. 4(c) we show the calculated spectrum for a conventional laser where the switching occurs above threshold. Two spectral peaks are observed, corresponding to the mark (at 1.5500 μm) and space (at 1.5501 μm). Even in this case the main modes are accompanied by small shoulders to the short (mark) and long (space) wavelength regimes. These shoulders and their positions relative to the main mark and space modes are again explained by the inevitable relaxation oscillation in the carrier density which accompanies the switching process. These calculations agree well and explain the results of Henmi *et al.*[3] who observed double peaked spectra and a large spectral spread in high bit rate directly modulated DFB laser diodes. The degree of spectral broadening and the subpeak to mainpeak intensity ratio are determined in part by the rise time of the imposed signal compared to the bit rate. It is clear that this ratio will be approximately given by τ_r/τ, where τ_r is the rise time of the modulation and τ is the inverse of the bit rate. Naturally, the broadening will also depend on the duration and decay time of the relaxation oscillations.

In conclusion, we have reported single-mode digital transmission over 8 km of fiber using an intracavity loss modulated MQW-DFB laser. We have shown the observed asymmetrical spectral broadening is due to carrier number oscillations which accompany the switching process. Conventional, digitally current-modulated lasers have broader linewidths than those which use a voltage-controlled intracavity loss modulator.

[1] K. Berthold, A. F. J. Levi, T. Tanbun-Ek, R. A. Logan, and S. N. G. Chu, Appl. Phys. Lett. **55**, 1940 (1989).
[2] A. F. J. Levi, R. N. Nottenburg, R. A. Nordin, T. Tanbun-Ek, and R. A. Logan, Appl. Phys. Lett. **56**, 1095 (1990).
[3] N. Henmi, S. Fujita, M. Yamaguchi, M. Shikada, and I. Mito, IEEE J. Lightwave Technol. **LT-8**, 936 (1990).
[4] J. O'Gorman, A. F. J. Levi, R. N. Nottenburg, T. Tanbun-Ek, and R. A. Logan, Appl. Phys. Lett. **57**, 968 (1990).
[5] T. Tanbun-Ek, R. A. Logan, H. Temkin, N. A. Olsson, A. M. Sergent, and K. A. Wecht, IEEE Photon. Technol. Lett. **2**, 453 (1990).
[6] Y. Arakawa, K. Vahala, and Y. Yariv, Surf. Sci. **74**, 155 (1986).
[7] N. K. Dutta, N. A. Olsson, and W. T. Tsang, Appl. Phys. Lett. **45**, 836 (1984).